Published in IET Optoelectronics
Received on 18th June 2013
Revised on 20th December 2013
Accepted on 6th January 2014
doi: 10.1049/iet-opt.2013.0076

ISSN 1751-8768

Efficient modulation technique for optical code division multiple access networks: differential pulse position modulation

Simin Khazraei, Mohammad Amin Shoaie, Mohammad Reza Pakravan

Electrical Engineering Department, Data Networks Research Laboratory, Sharif University of Technology
E-mail: khazraei_s@yahoo.com; khazraei@ieee.org

Abstract: In this study, the authors study a fibre-optic local area network deploying optical code division multiple access technique with differential *M*-ary pulse position modulation (DPPM). The authors present the performance analysis of DPPM signalling using a double optical hardlimiter receiver structure considering the impairment caused by interference of other users. The analysis assumes a set of bit asynchronous transmitters employing generalised optical orthogonal codes for their DPPM signalling (GOOC-DPPM). Using mathematical analysis and simulations, the authors have demonstrated that GOOC-DPPM improves both frame error probability and the maximum achievable network throughput compared with *M*-ary PPM modulation scheme. It is also indicated that using generalised OOC codes instead of strict OOC codes in DPPM modulation can increase the number of users who can simultaneously transmit data in the network. The authors have analysed the stability of GOOC-DPPM in a multi-user system and demonstrated its stability. Moreover, the performance of the proposed scheme is evaluated when its important design parameters such as code length, code weight and multiplicity index of the modulation are changed. The findings led the authors to provide some guidelines for proper selection of these parameters to be used for efficient system design.

1 Introduction

Optical code division multiple access (OCDMA) is an appropriate solution to satisfy the needs in a local area network (LAN) [1–3]. 'Soft capacity', 'no unnecessary synchronisation between users' and 'system simplicity' are among the advantages of code division multiple access (CDMA) over other multiple access techniques, such as time division multiple access (TDMA) and wavelength division multiple access (WDMA) [4]. The large bandwidth and high-speed optical signal processing offered by optical components enables OCDMA systems to accommodate a large number of active users simultaneously [5–7]. In this respect, optical orthogonal code (OOC) is a well-designed technique which implements CDMA in the optical domain [6–8]. OOC is highly viable and important in some optical communication systems as also verified in [9]. In fact, an OOC is a signature code with a chip length of L and a code weight of w, which satisfies the maximum auto- and cross-correlation interference values denoted by $\lambda_a = \lambda_c = \lambda$. Besides, Mashhadi [8, 10] has shown that, having a larger cross-correlation, generalised OOCs, ($\lambda > 1$), outperforms strict OOCs with $\lambda = 1$.

Among various modulation techniques, on-off keying (OOK) and pulse position modulation (PPM) are popular methods which are used in intensity modulation/direct detection optical communication systems. It has also been proved that PPM is more favourable in power-limited networks in comparison with OOK [5, 11–13]. However, since *M*-ary PPM is a sparse signalling technique, it appears not to be efficient in terms of throughput. In this regard, Shalaby has investigated overlapping PPM (OPPM) technique, in which a fixed overlap was introduced between adjacent PPM slots in order to increase the bandwidth efficiency of this scheme. He also demonstrated that this method is of great advantages compared with OOK modulation technique [14, 15]. OPPM with generalised OOC is analysed in [16, 17]. Yet an alternate technique to enhance PPM bandwidth efficiency is differential PPM (DPPM) signalling, which is extracted from PPM by omitting zero slots after each pulse [18, 19]. In his study, Kahn has proved that this technique outperforms PPM in indoor wireless infrared communications where the channel has additive white Gaussian noise.

In this paper, for the first time to our knowledge, we analyse DPPM signalling scheme in an OOC based fibre-optic multiple access network. We consider double optical hardlimiter as the receiver structure and multiple access interference (MAI) as the dominant limiting factor. The analysis is presented for the general case of asynchronous data bits coded by generalised OOCs (GOOCs). This provides an analytical framework for further studies on error correction techniques and analysing more complex signallings. An evaluation of the system performance indicates significant improvement in the maximum achievable throughput and bit error rate, in comparison with

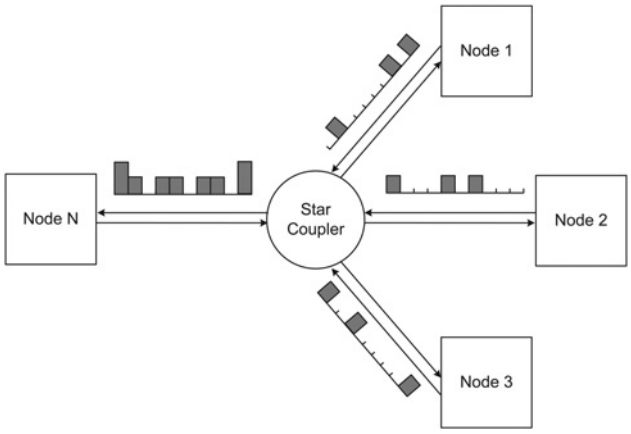

Fig. 1 *LAN with N users communication through a star coupler employing GOOC-DPPM*

those obtained from PPM technique. System stability is an important issue in network design. Stability of the system is also discussed. The effects of code and modulation parameters on system performance were also evaluated and a number of guidelines were proposed for proper selection of these system parameters. The rest of this paper is thus organised as follows. Section 2 presents a description of the system and DPPM signalling. In Section 3 we derive the performance of GOOC-DPPM network. Stability analysis is discussed in Section 4. The numerical results are reported in Section 5 and guideline for parameter selection is provided in Section 6. Finally, the paper is concluded in Section 7.

2 System description

The network we have considered here is a LAN which consists of N active users communicating over optical fibre through a star coupler (Fig. 1). In such a network, distances are short and therefore the loss is low and thus fibre dispersion can be ignored. Each of the users are assigned a unique GOOC as their signature code. In this system, data bits are coded by the DPPM signalling scheme, which is a modified version of PPM technique. In M-ary PPM signalling, having the symbol length of M slots, the desired symbol is conveyed by inserting a pulse at the specified slot whereas other slots are set to zero. DPPM signalling is extracted from PPM by deleting zero slots after each pulse. It has to be noted that in the OOC based system, the pulse slot is modulated by the corresponding GOOC. Fig. 2 depicts DPPM symbols using OOC with multiplicity index, $M = 4$, and code parameters $L = 9$, $w = 3$ and $\lambda = 1$. The minimum and maximum lengths of a DPPM symbol are 1 and M slots, respectively. PPM symbols are also depicted in Fig. 2 for comparison.

Conventional error correcting codes cannot directly be applied to DPPM systems because of variable length symbols, which leads to insertion/deletion errors [20, 21]. In our system architecture, which is a LAN and users are not too far from each other, the fibre-optic path loss is negligible. Therefore if a transmitter sends an optical pulse in a particular chip time, the receiver detects energy in that chip position. On the other hand, if a transmitter does not send an optical pulse in a particular chip time (meaning '0' in that chip), the receiver detects no energy if there is no interference and detects some energy if there is interference from the transmitted pulses of other transmitters during that particular chip. That causes the receiver to detect a transmitted '0' chip as a '1' chip. This can lead to an error in proper detection of a slot which in turn may result in the detection of an extra symbol by the receiver. In other words, in this DPPM-GOOC system, there is only insertion errors and no deletion errors. In this system, a mis-detected slot can lead to insertion of an extra symbol in the data stream, which shifts all of its following symbols and therefore there is an error propagation mechanism that is to be controlled [21]. To remedy this situation, we propose to divide the bit stream into separate frames and prevent long

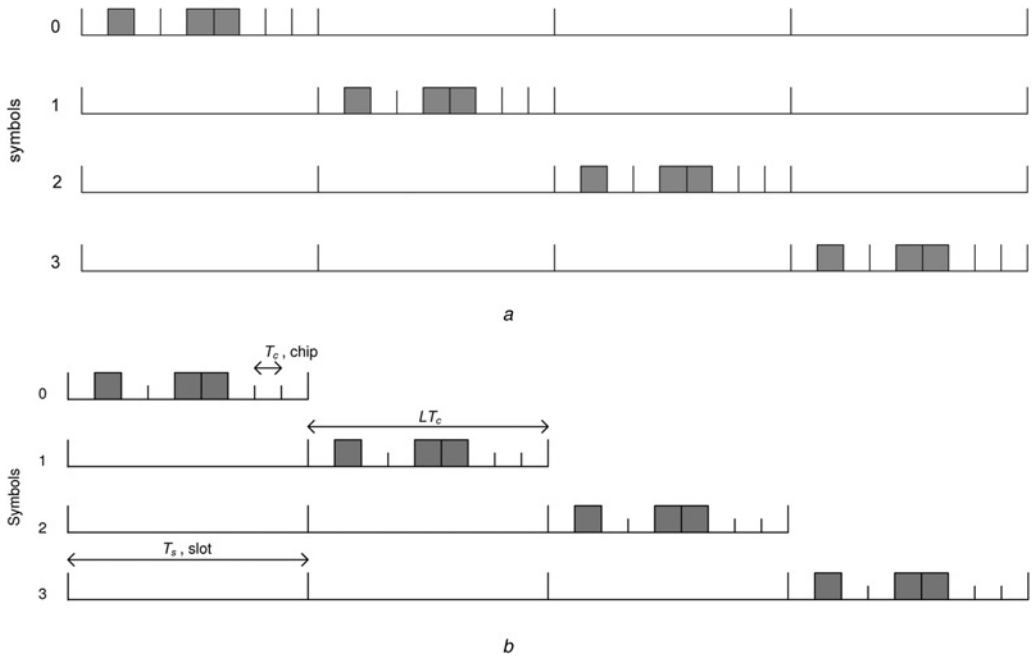

Fig. 2 *Signalling schemes with multiplicity index = 4 and code parameters, L = 9, w = 3 and λ = 1*

a PPM
b DPPM

doi: 10.1049/iet-opt.2013.0076

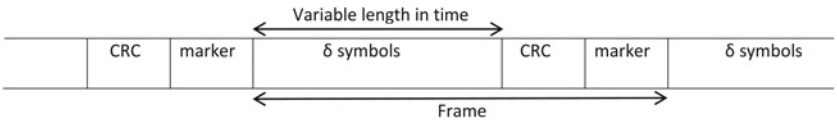

Fig. 3 *Frame is composed of δ data symbols, CRC and a marker*
Data length is variable in time

term error propagation by separating frames with proper markers. If there is an error in a frame, only that frame will be affected and the error will not be propagated to the next frame, which thus improves the system performance [20]. A marker is inserted every δ symbols. The marker itself is an OOC with duration equal to one slot (a slot is illustrated in Fig. 2).

Two codes are assigned to each user, one standing for the data and the other indicating frame marker. In case a particular OOC is used as the marker of all users, there is a considerable chance that the marker of an interfering user is received during a '0' slot of a symbol of the desired user and causes mis-detection of the frame boundary. That is why we propose to use a separate marker code for each user. Moreover, a cyclic redundancy check (CRC) is placed before the marker in each frame. A frame is a set of δ data symbols, CRC and a marker as illustrated in Fig. 3. It is noteworthy here that the data symbol length is variable as the DPPM symbols are of different lengths. Hence, it is the CRC that helps the receiver realise whether the frame is received correctly or not.

The receiver has two branches, one of which detects data and the other is used to detect the frame marker. The structure of the receiver structure is presented in Fig. 4. Each detector is a double optical hardlimiter which is an all optical implementation of the chip level detector [8, 22]. The optical hardlimiter threshold is denoted by Th. For a given input value x, output y is denoted by the rule

$$y = \begin{cases} 1 & x \geq \text{Th} \\ 0 & x < \text{Th} \end{cases} \tag{1}$$

Each decoder determines whether there exists a '1' (*one* slot) or a marker in each slot. The output is converted to electrical signal and enters an electrical decision block which decides about the received symbol according to the number of zero slots between one slots.

3 Performance analysis of the GOOC-DPPM system

To analyse the performance of the GOOC-DPPM system, we start with calculating the error probability of a frame. CRC indicates the number of CRC bits in a frame. Since every $\log_2 M$ bits corresponds to one DPPM symbol, exactly like PPM [5], the ceil of (CRC/$\log_2 M$) represents the number of symbols added to a frame because of CRC bits

$$\beta = \delta + \left\lceil \frac{\text{CRC}}{\log_2(M)} \right\rceil \tag{2}$$

where $\lceil\rceil$ represents ceil and β is the total number of symbols in a frame, including data and CRC. Define

$$\mu = M - 1 \tag{3}$$

μ is the maximum number of *off* slots in a symbol and therefore $\mu\beta$ is the maximum possible number of *off* slots in a frame. Probability of error in a frame is denoted by P_{frame}. This probability is obtained by averaging over the number of *off* slots in that frame

$$P_{\text{frame}} = \sum_{k=0}^{\mu\beta} P(\text{error in the frame}|k \text{ off slots}) \times P(k \text{ off slots}) \tag{4}$$

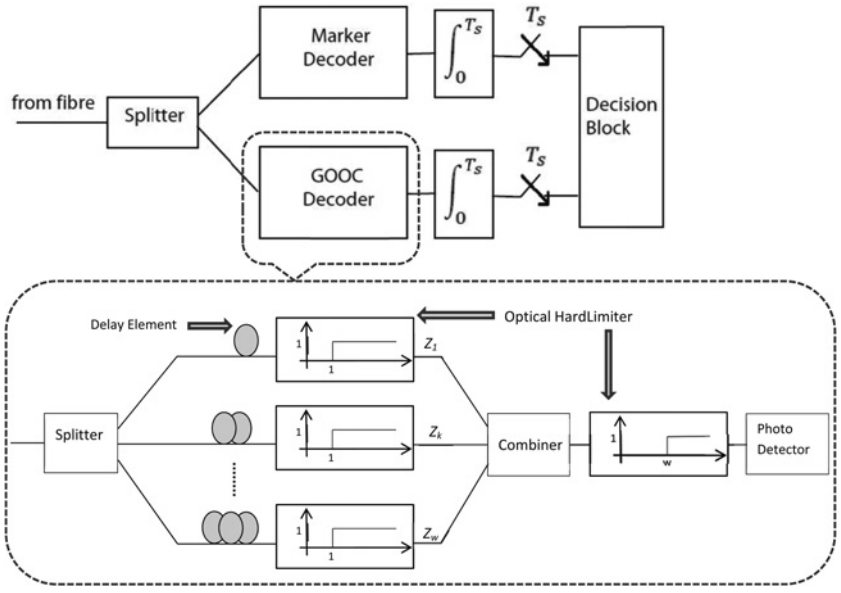

Fig. 4 *Receiver structure of GOOC-DPPM*

Each symbol may have 0,1, 2, …, $M-1$ *off* slots. We call the number of *off* slots in each symbol by K_i. K_i's are random variables uniformly distributed between 0 to μ with mean ($\mu/2$) and variance ($\mu^2+2\mu$)/12

$$K_1 + K_2 + \cdots + K_\beta = K \tag{5}$$

K itself is a random variable with mean ($\mu\beta/2$) and variance (($\mu^2+2\mu)\beta/12$). When β is large, sum of β i.i.d. random variables can be approximated by a normally distributed variable using central limit theorem with mean and variance as stated above [23]. Hence

$$P(K=k) = C\phi\left(\frac{k-(\mu\beta/2)}{\sqrt{((\mu^2+2\mu)\beta/12)}}\right) \tag{6}$$

ϕ is the pdf of standard normal distribution and C is the normalising constant

$$\sum_{k=0}^{\mu\beta} C\phi\left(\frac{k-(\mu\beta/2)}{\sqrt{((\mu^2+2\mu)\beta/12)}}\right) = 1 \tag{7}$$

where $\mu\beta$ is the maximum number of *off* slots in a frame

$$C = \frac{1}{\sum_{k=0}^{\mu\beta}\left(1/\sqrt{2\pi}\right)\mathrm{e}^{-\left(6(k-(\mu\beta/2))^2/(\mu^2+2\mu)\beta\right)}} \tag{8}$$

In an optical fibre LAN with many users using OOC codes, MAI is the dominant performance limiting factor if sufficient power is assumed in receivers. As mentioned before, the interference induced errors, cause some *off* slots to be detected as one or marker. Note that one slots may also be detected as a marker mistakenly. Receiver follows these steps to detect a frame

- Each slot is detected separately.
- When a marker is detected, receiver counts the number of symbols between the newly received marker and the previous marker. If there exists δ symbols and CRC is correct, the frame is reported as correct. Otherwise, the frame is reported as error.

In some cases, an extra (or more) marker is detected in a frame because of MAI and the frame is divided in two (or more) parts. The parts which have less than δ data symbols, are all reported as error. In some rare conditions, interference from other users may cause some *off* slots to be detected as *one* and the insertion of symbols in that part causes the receiver to think that it has detected δ data symbols. We have used CRC to detect these types of errors as well. The probability that an incorrect set being accepted as valid, is ignorable. The probability of error in a frame that consists of k *off* slots is

$$\begin{aligned} &P(\text{error in the frame}|k \text{ off slots}) \\ &= 1 - P(\text{the frame is correct}|k \text{ off slots}) \end{aligned} \tag{9}$$

A frame is correct if all *one* and *off* slots and also the marker are detected correctly. Since slots are independent in DPPM

$$\begin{aligned} &P(\text{the frame is correct }|k \text{ off slots}) \\ &= P(\text{all off slots are correct }|k \text{ off slots}) \\ &\quad \times P(\text{all one slots are correct }|k \text{ off slots}) \end{aligned} \tag{10}$$

$$\begin{aligned} &P(\text{all off slots are correct }|k \text{ off slots}) \\ &= \left[1 - P(\text{an off slot is incorrect})\right]^k \end{aligned} \tag{11}$$

An *off* slot is incorrect if it is detected as *one* or as a marker. Since these probabilities are correlated, we use the upper bound on error probability

$$\begin{aligned} &P(\text{an off slot is incorrect}) \\ &\le P(\text{an off slot is detected as a one}) \\ &\quad + P(\text{an off slot is detected as a marker}) \end{aligned} \tag{12}$$

The probabilities that an *off* slot be detected as different OOCs are the same; hence

$$\begin{aligned} &P(\text{an off slot is detected as a one}) \\ &= P(\text{an off slot is detected as a marker}) = q_0 \end{aligned} \tag{13}$$

Therefore

$$P(\text{all off slots are correct }|k \text{ off slots}) = [1-2q_0]^k \tag{14}$$

q_0 is the probability that an OOC decoder, detects an *off* slot as *on*

$$q_0 = \sum_{m=1}^{N-1}\binom{N-1}{m} p_i^m (1-p_i)^{N-m-1} p_e(m) \tag{15}$$

here, p_i is the probability that an interfering user interferes with an *off* slot of the desired user in GOOC-DPPM system and $p_e(m)$ denotes the probability that the desired user misreads the *off* slot as *on* whereas m interfering users are present. In Appendix 1, p_i is derived as

$$p_i = \frac{1}{M}$$

Fig. 4 shows the receiver structure. An *off* slot will be detected as *one* if all the variables Z_1, Z_2, …, Z_w equal to one. This means that if any of the variables equals to zero, the slot is correctly detected. When any of the variables equals to zero, the product $Z_1Z_2 \ldots Z_w$ equals to 0

$$\begin{aligned} p_e(m) &= 1 - P(Z_1Z_2\ldots Z_w = 0|m) \\ P(Z_1Z_2\ldots Z_w = 0|m) &= \sum_{k=1}^{w}(-1)^{k+1}\binom{w}{k}P(Z_1\ldots Z_k = 0|m) \\ p_e(m) &= 1 + \sum_{k=1}^{w}(-1)^{k}\binom{w}{k}P(Z_1\ldots Z_k = 0|m) \end{aligned} \tag{17}$$

In a system employing generalised OOC, the probability that k chip pulse positions does not suffer from interference when there exists m interfering users, can be obtained similar to

doi: 10.1049/iet-opt.2013.0076

OOK, as in [8]

$$P(Z_1 \ldots Z_k = 0|m) = \left[1 - \sum_{n=1}^{\lambda} \frac{wt_n}{n} \binom{w-1}{n-1} \left(1 - \frac{(w-n)(w-n-1)\ldots(w-n-k+1)}{w(w-1)\ldots(w-k+1)}\right)\right]^m \quad (18)$$

where t_n is the probability that an *on* slot of a user interferes at n chip pulse positions on the *off* slot of the intended user. There are w^2 chip pulse positions that an interfering user can hit, on L possible chip positions. Therefore total probability that a chip pulse position of an *on* slot of an interfering user interferes with any of chip pulse positions of an *off* slot of desired user equals to w^2/L

$$\sum_{k=1}^{\lambda} k \binom{w}{k} t_k = \frac{w^2}{L} \quad (19)$$

Consider the worst case where all interferers interfere at λ chip pulse positions; $t_j = 0$, where $j = 1, \ldots, \lambda - 1$ and $t_\lambda \neq 0$, hence, (18) reduces to

$$P(Z_1 \ldots Z_k = 0|m) = \left[1 - \frac{w^2}{\lambda L}\left(1 - \frac{(w-\lambda)(w-\lambda-1)\ldots(w-\lambda-k+1)}{w(w-1)\ldots(w-k+1)}\right)\right]^m \quad (20)$$

Finally

$$p_e(m) = 1 + \sum_{k=1}^{w} (-1)^k \binom{w}{k} \left[1 - \frac{w^2}{\lambda L}\left(1 - \frac{(w-\lambda)(w-\lambda-1)\ldots(w-\lambda-k+1)}{w(w-1)\ldots(w-k+1)}\right)\right]^m \quad (21)$$

For data *one* slots

$$P(\text{all one slots are correct } |k \text{ off slots}) = [1 - q_1]^\beta \quad (22)$$

β is the total number of *one* slots in a frame and $q_1 = P(\text{an one slot be detected as marker})$. q_1 is calculated similar to q_0 noting that the *one* slot itself behaves like an extra interferer on the slot to be detected as marker

$$q_1 = p_e(1) + \sum_{m=1}^{N-1} \binom{N-1}{m} p_i^m (1 - p_i)^{N-m-1} p_e(m+1) \quad (23)$$

Finally we have

$$P(\text{error in the frame } |k \text{ off slots}) = 1 - [1 - 2q_0]^k [1 - q_1]^\beta \quad (24)$$

By substituting (24) in (4), probability of frame error, P_{frame}, of GOOC-DPPM is obtained

$$P_{\text{frame}} = \sum_{k=0}^{\mu\beta} \left(1 - [1 - 2q_0]^k [1 - q_1]^\beta\right) P(k \text{ off slots}) \quad (25)$$

Probability of k *off* slots is also obtained in (6) and (8), and finally we have

$$P_{\text{frame}} = \sum_{k=0}^{\mu\beta} \left(1 - [1 - 2q_0]^k [1 - q_1]^\beta\right) \times \frac{1}{\sum_{k=0}^{\mu\beta} (1/\sqrt{2\pi}) e^{-(6(k-(\mu\beta/2))^2/(\mu^2+2\mu)\beta)}} \phi \times \left(\frac{k - (\mu\beta/2)}{\sqrt{((\mu^2 + 2\mu)\beta/12)}}\right) \quad (26)$$

4 Stability analysis

Users may not be active all the time in a LAN. They transmit their new frames with probability p_0. Some of these frames may encounter collisions with the frames of other users and all collided frames will not be usable for their target destinations. In the performance analysis section, we have calculated the probability of a frame being received with errors. It is assumed that frames should be completely error-free for proper detection and even a single bit of error requires re-transmission of the frame by media access control (MAC) sublayer. Let us assume that the probability that a frame will be retransmitted is denoted by p_r. In such a network, if MAC parameters are not set properly, the system may become unstable or even bistable [16]. This means that all the users may become busy retransmitting their old frames, and no new frame can be transmitted. For this reason, we briefly discuss the stability of the system. For simplicity, we assume that MAC layer of the system has some specific time intervals denoted by Δ and whenever a user has some frames, it sends it at the start of this time frame (concept of slotted MAC). Assume that Δ is equal to the maximum length of a frame. Users who have sent their frames successfully, are in *origination* mode. Any user whose recent frame is destroyed because of MAI should re-transmit its frame and is *backlogged*. The system can be modelled using Markov model and system state which is denoted by x_t is defined as the number of *backlogged* users at time t. Dynamic behaviour of x_t is given by a Markov chain with a stationary transition matrix and $N+1$ states corresponding to 0,...,N backlogged users [16, 24]. The value of x_t changes because of unsuccessful new transmission (U-NTX) that increases this value and successful re-transmissions (S-RTX) that decreases its value. We define $b(\alpha, n, \rho) \triangleq \binom{n}{a} \rho^\alpha (1-\rho)^{n-\alpha}$. The probability of k successful retransmission and l U-NTX when the number of backlogged users equals n is given by [24]

$$Pr\{\text{S}-\text{RTX} = k, U-\text{NTX} = l | x_t = n\} = \sum_{\xi_0=l}^{N-n} \sum_{\xi_r=k}^{n} b[l, \xi_0, P_E(\xi_0 + \xi_r)].b[k, \xi_r, P_c(\xi_0 + \xi_r)] b(\xi_0, N-n, p_0).b(\xi_r, n, p_r) \quad (27)$$

where $P_c(a)$ is the probability of a frame being received correctly when there are a users in the network and $P_E(a) = 1 - P_c(a)$. p_{nm} represents the probability of transition from state n to m. Note that a state transition from n to m, for $n \geq m$ happens when number of {U-NTX} exceeds {S-RTX} by $n - m$ and for $n < m$ when number of {S-RTX} exceeds {U-NTX} by $m - n$ [16]. Hence, $p_{nm} = \Pr\{x_{t+1} = m | x_t = n\}$, is obtained by

$$p_{nm} = \begin{cases} \sum_{j=0}^{\min(n,N-m)} \Pr\{S - \text{RTX} = \text{j},\ U - \text{NTX} \\ \quad = m - n + \text{j} | x_t = n\} \text{ for } m \geq n \\ \sum_{j=0}^{\min(m,N-n)} \Pr\{S - \text{RTX} = n - m + \text{j} \\ \quad U - \text{NTX} = \text{j} | x_t = n\} \text{ for } m \leq n \end{cases} \quad (28)$$

Dynamic behaviour of the system can be analysed using expected drift which is defined by [25]

$$d(n) = \sum_{m=0}^{N} (m - n) p_{nm} \quad (29)$$

Any state where $d(n)$ is small and close to zero, is a stable state, because the random walk defined in (29) has the least tendency to move forward or backward. An equilibrium point is stable if expected drift crosses state axis with negative slope [24]. This means that if the value of the system state increases (decreases), the system has a tendency to decrease (increase) that value because the expected drift is negative. Stability of the GOOC-DPPM system is provided in the next section.

5 Numerical results

In this section, the numerical results of the analysis are being provided to shed more light on the performance of OCDMA system based on DPPM. The results are obtained from the analytical equations derived in the previous section. Comparisons are also made against the results yielded by the GOOC-PPM technique which is analysed in [16, 17].

In the following plots, there are several system parameters, each of which is to be determined individually:

- M: The multiplicity index of M-ary signalling.
- N: The number of active users in network.
- L: The length of GOOC in chips.
- w: The GOOC code weight.
- λ: The cross-correlation value of GOOC set.

Among the above mentioned parameters, in each plot M, N and λ are treated as independent variables. We define the other parameters in a way that the comparison is fair. The chip duration T_c is kept constant to make sure that all systems use the same bandwidth. Yet another factor is the amount of information per chip, that is, R_0, conveyed by users. In M-ary PPM signalling, R_0 is obtained by $\log_2 M/L/M$. Note that in DPPM, each $\log_2 M$ bits, which is equal to one symbol, occupies $(M+1)/2$ slots on average. In order to consider the effects of δ and CRC, we note that each δ symbols are followed by (CRC $(M+1)/(2 \log_2 M)$) slots for CRC and one slot for marker. Each slot is composed of L chips. Thus $\delta \log_2 M$ bits are transmitted using $L(\delta(M+1/2) + 1 + (\text{CRC}(M+1)/(2 \log_2 M))$ chips. Therefore the amount of information transmitted in a chip time, or R_0, is equal to

$$R_0 = \frac{\delta \log_2 M}{L\left(\delta(M + 1/2) + 1 + \left(\text{CRC}(M+1)/(2 \log_2 M)\right)\right)} \quad (30)$$

These conditions assure equal bandwidths and bit rates in all schemes. Thus, for any signalling, we simply need to determine L, using the corresponding R_0 value. Therefore having the N, L and λ, the GOOC code weight is calculated based on Johnson bound in (31)

$$N(L, w, \lambda) \leq \left\lfloor \frac{(L-1)(L-2)\ldots(L-\lambda)}{w(w-1)\ldots(w-\lambda)} \right\rfloor \quad (31)$$

$\lfloor\rfloor$ represents floor (integer part of the value). Using (31), we select the maximum allowable w, so that all code sets equally utilise the highest GOOC capacity. We assume a system with $\delta = 100$ symbols between markers and an eight bit CRC. R_0 is equal to 4×10^{-3} and the other parameters are shown in figures.

In order to verify the analysis, simulation was performed. The parameters were set as follows: $L = 63$, $w = 5$, $\lambda = 2$ and $M = 8$. We generated the code set using the *greedy algorithm*, and two OOCs were assigned to each user. The *greedy algorithm* is a well-known method to construct OOCs [26]. Fig. 5 presents a comparison between the analytical and simulation results. Analytical results are an upper bound on the simulation results. In the analysis, we considered the upper bound used in (12). Equation (18) is also regarded as an upper bound as it considers the worst case where all the interferences from other users are in λ chip positions. Yet it has to be noted that interference from other users varies from 0 to λ chip positions. This upper bound is not tight when N is low [27]. In the following figures, only the analysis (which results in an upper bound on the frame error) is considered. Thus the actual results would be much better than what is presented here.

Comparing M-ary PPM and DPPM signalling, Fig. 6 depicts the frame error probability P_{frame}, against the number of active users for two multiplicity index values.

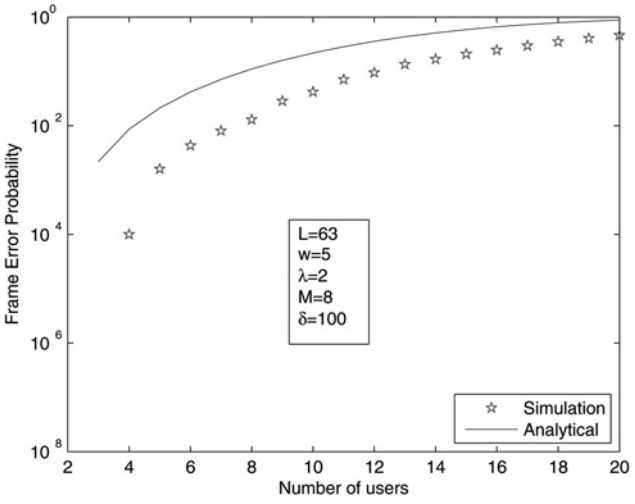

Fig. 5 *P_{frame} obtained from analysis and simulation*

Analytical results are an upper bound on simulation results, because we considered the worst case in the analysis

doi: 10.1049/iet-opt.2013.0076

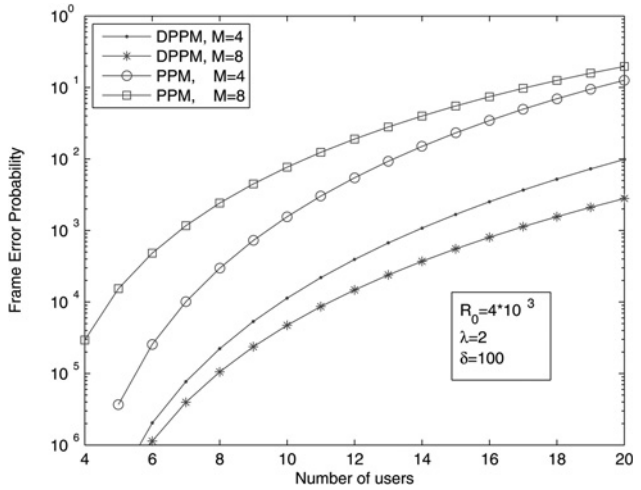

Fig. 6 *P_{frame} against number of users for PPM and DPPM*

The plots show that for both cases of $M = 4$ and 8, DPPM technique has lower P_{frame} compared with PPM (although we extracted an upper bound on the frame error rate). For example, when M is equal to 8, the frame error rate (FER) of PPM signalling is approximately 10^{-1}, whereas DPPM has an FER equal to 10^{-3}, which is about 100 times lower than that of PPM. It should be noted that we have used two codes for each user in DPPM (one for data transmission and the other for marker), and consequently longer codes should be used to support the same number of users. Despite this fact, eliminating *off* slots in DPPM symbols compensates for larger code sizes and results in lower FER compared with PPM. Furthermore, to maintain P_{frame} below 10^{-3}, PPM supports seven users whereas DPPM allows 16 users to transmit simultaneously. Remember that both systems use the same bandwidth, transmit an equal amount of information per chip time and the effect of marker and CRC are also taken into account, which appear in R_0.

Fig. 7 illustrates a comparison between strict OOC and generalised OOC. It can be viewed that, using GOOC, DPPM outperforms strict OOC where $\lambda = 1$. As an example, when there are 20 users in the network, DPPM with $\lambda = 3$ has three orders of magnitude lower FER compared with $\lambda = 1$. In addition, when $P_{\text{frame}} < 10^{-4}$, DPPM with strict OOC supports ten users, whereas $\lambda = 3$ supports more than 20 users. This implies that generalised OOC can increase the number of users who can simultaneously transmit data in the network. Besides, for $\lambda = 3$, when P_{frame} is about 10^{-4}, DPPM supports 20 users, whereas PPM supports less than ten users.

One of the fundamental figures of merit is spectral efficiency which is defined as the total number of bits per chip that can be transmitted by all the users in the system [28]. In a CDMA system, the bandwidth is roughly equal to the inverse of the chip duration. Therefore the spectral efficiency defined above is the total number of bits per second per Hertz (bits/s/Hz) transmitted by the system. Spectral efficiency, or total throughput, can thus be regarded as the product of the number of users and the amount of information delivered by each user in a chip time (R_0)

$$S_{\max} = NR_0(\text{bits/s/Hz}) \tag{32}$$

In order to study spectral efficiency, we find codes that are long enough to allow the P_{frame} to be below 10^{-3}. Fig. 8 demonstrates spectral efficiency, $S_{\max}$, against N, for DPPM signalling. This figure shows that DPPM has a better spectral efficiency compared with PPM, as the number of users grow. Note that the effects of inserting a marker and CRC are taken into account as well. The advantage of GOOC-DPPM is that it has fewer empty time slots and therefore its average symbol duration is shorter and achieves a higher efficiency in using time for transmission of information. Fig. 9 illustrates the effect of M on the spectral efficiency. In this figure, spectral efficiency is plotted against M, for different values of λ and various number of users. According to this figure, there exists an optimum value for M which has the highest spectral efficiency.

Yet another factor affecting system performance is the number of symbols inserted between two markers which is shown by δ. When δ is low, the channel is mostly busy sending the marker and therefore the bandwidth is used inefficiently. On the other hand, if δ is large, the probability of frame error increases. Hence, the value of δ should be chosen properly to optimise the system performance. Fig. 10 illustrates FER against δ for different values of N. In this figure, for each number of users, there exists an optimum value for δ ($\delta = 100$) which minimises FER.

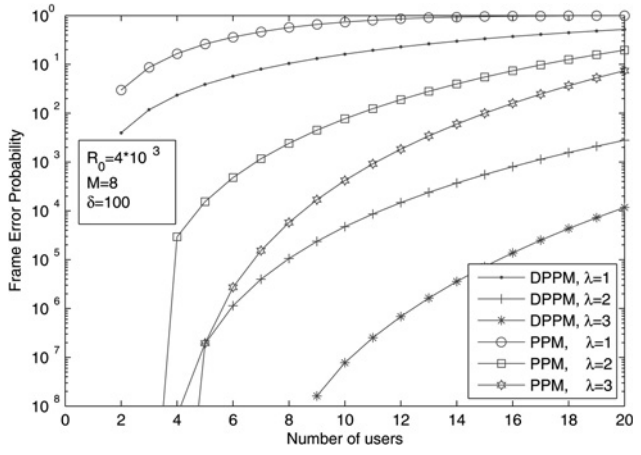

Fig. 7 *Frame error probability against the number of users for different values of λ*

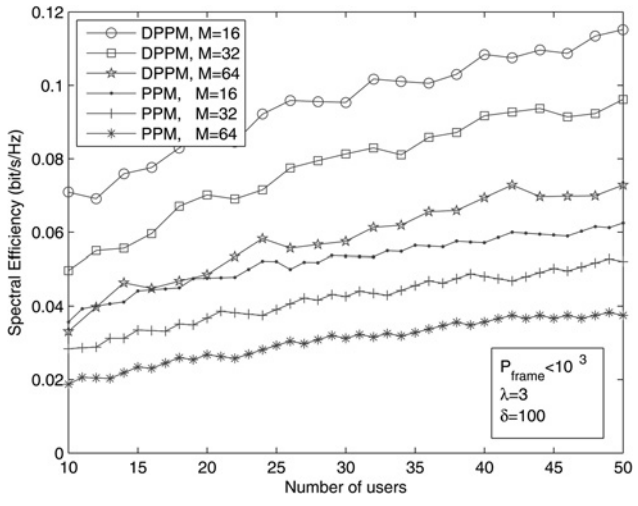

Fig. 8 *Spectral efficiency of DPPM against number of users*

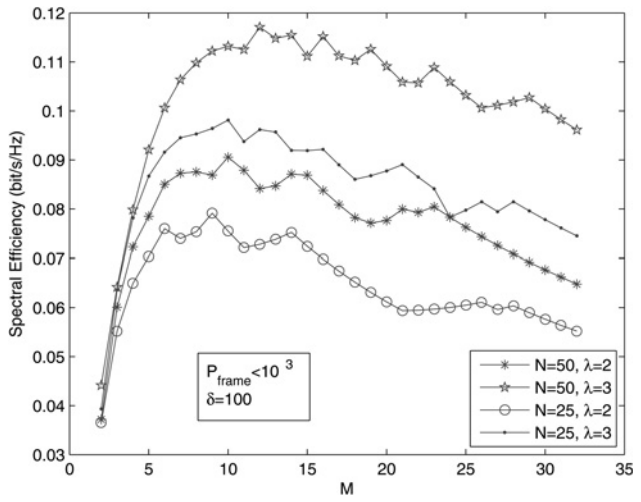

Fig. 9 *Effect of M on spectral efficiency of DPPM*

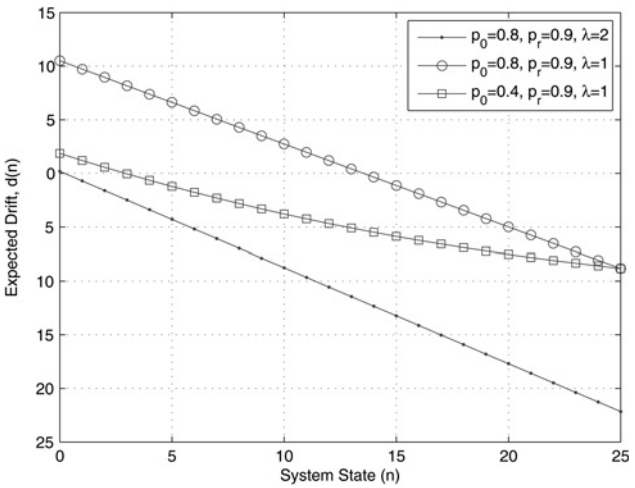

Fig. 11 *Expected drift of a system employing DPPM*
In all cases, the network is stable

In a LAN, users are not active all the time. They transmit their new frames with probability p_0 and retransmit their failed frames with probability p_r. If probability of error in a frame is high, users are most of the time busy retransmitting their frames. In this case, the network may become unstable or bistable. Fig. 11 illustrates expected drift against system state with parameters $R_0 = 4*10^{-3}$, $M = 8$, $N = 25$, $\delta = 100$ and CRC = 8. Two cases is considered: $p_0 = 0.4$ and 0.8.

The latter is an example of a crowded network. This figure shows that in both cases, crowded or not, system has just one stable equilibrium point. When $p_0 = 0.4$, system is stable with five users backlogged in the network. However, when p_0 equals to 0.8, 15 users are backlogged most of the time. Totally, proper selection of system parameters, makes the system stable.

6 DPPM OCDMA parameter selection

In this section, we introduce a systematic code design algorithm that can be used to find the suitable set of code and signalling parameters to increase network resource utilisation. An important question in a system design process, is 'what is the best code set, (L, w, λ), and multiplicity index, M, to achieve a good throughput when number of users is known?' In response this question, the total throughput (spectral efficiency) of the system is calculated for all values of M and λ, provided that the probability of frame error is less than 10^{-6}. Code length, or L, is increased up to the value where the probability of frame error falls below 10^{-6}. Code weight is also determined using Johnson bound, eq. (31). Finally, we search for the values of M and λ which maximise throughput. The design algorithm will be described below in details.

To clarify the procedure, we start with an example. As the first step, the throughput should be plotted against N and M as a three-dimensional graph for different values of λ. Using this graph, we compare the performance of system using different λs and can thus determine the best value of λ. A better way for comparison, is to define ξ_{21} = throughput($\lambda = 2$) – throughput ($\lambda = 1$). A positive ξ implies that $\lambda = 2$ outperforms $\lambda = 1$. Fig. 12 portrays ξ_{21} against M and N. It can be observed from the figure that ξ_{21} is positive for all values of M and N. This indicates that when there are 10–50 users in the network, for any value of M, the system using codes with $\lambda = 2$ shows a better performs than the system with $\lambda = 1$.

It has to be noted that, in our comparison between cross-correlations (λ), for each N, it is sufficient to compare

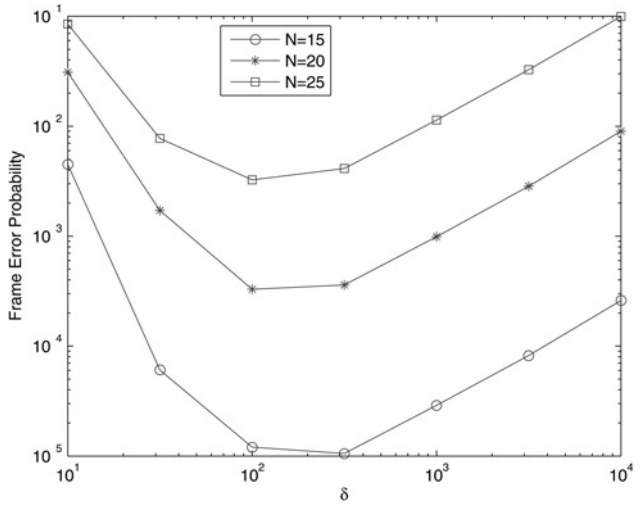

Fig. 10 *Spectral efficiency for different values of δ*

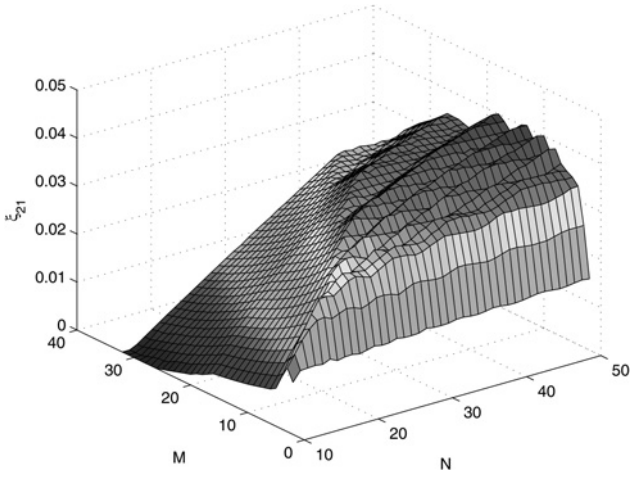

Fig. 12 *Comparison of throughput when λ = 1 and 2*

doi: 10.1049/iet-opt.2013.0076

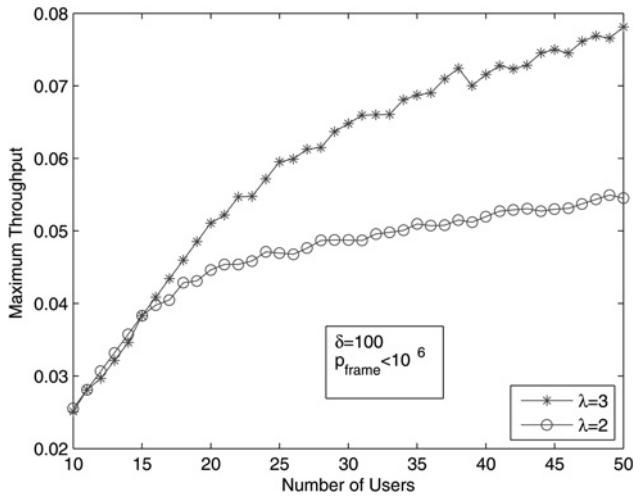

Fig. 13 *Comparison of maximum throughput for each number of users when λ = 3 and 2*

M is selected in such a way to maximise throughput.

throughputs in optimum points, that is, the optimum multiplicity index, *M*, which maximises the throughput. Therefore in order to compare system performance in the cases of $\lambda = 2$ and 3, we simply extract optimum *M* which maximises the throughput, and compare the maximum throughputs. This results in a two-dimensional graph, in which throughput is plotted against *N*. In each point, *M* is selected to maximise the throughput. Fig. 13 illustrates the maximum throughput of the system for each number of users when $\lambda = 2$ and 3. As can viewed in this figure, when there are more than 15 users in the network, $\lambda = 3$ yields a better throughput compared with $\lambda = 2$. For a number of 10–15 users, $\lambda = 2$ and 3 have similar performances, therefore we continue with $\lambda = 3$. Code length, or *L*, is determined to ensure $P_{\text{frame}} < 10^{-6}$. Code weight is also calculated using Johnson bound (31). The optimum values for *M*, *L* and *w* are reported in Table 1. These values are provided as an example when there are 10–50 users in the network.

The parameter selection algorithm for a known number of users can be summarised as follows:

1. Consider all the possible values for *M* and λ.
2. In each case, assume a wide range for *L*.
3. For each *L*, calculate *w* using (31) for a known number of users.
4. Calculate P_{frame} for the codes considered in steps 2 and 3 using (26).
5. The shortest code set which satisfies $P_{\text{frame}} < 10^{-6}$ is considered as the best code set, as it increases R_0, (30).
6. Estimate the throughput using (32) for the code set selected in step 5.
7. Repeat steps 2–6 to extract the throughput for all values of *M* and λ.
8. Plot the throughput against *M* for different values of λ.
9. Now you can decide on the optimum values of *M* and λ which maximise the throughput!

Table 1 Optimum values for *M*, *L* and *w*

Number of users	*M*	*L*	*w*
10	4	160	22
20	4	289	29
30	8	300	27
40	8	365	29
50	8	420	30

7 Conclusion

Performance analysis of a fibre-optic LAN using GOOC-DPPM system has been studied. In these networks, there are many users who transmit data in the network simultaneously. Each user has a detector with a double optical hardlimiter structure. We analysed the system performance and obtained the frame error probability of *M*-ary DPPM, considering the MAI as the dominant source of detection impairment. In this network, data stream is divided into frames, each of which consists of δ DPPM symbols, a marker and a CRC whose effects on system performance has also been considered in all analysis. It was revealed from the results that DPPM technique provides substantial improvement in terms of both frame error rate and spectral efficiency, when compared with PPM. As an example, when $M = 8$ and $\lambda = 2$, DPPM has two orders of magnitude lower frame error rate compared with PPM. It was also found that DPPM increases the number of active users in the network. For instance, when frame error rate is less than 10^{-3}, PPM supports seven users, where as DPPM allows 17 simultaneous users. We analysed the stability of this system in a multi-user shared channel environment when an Abramson's logic of hiring access (ALOHA)-type multiple access control mechanism is used. We demonstrated that when proper set of parameters are chosen, the GOOC-DPPM is stable and has just one stable equilibrium point. In addition, we evaluated the performance of the proposed scheme for various values of design parameters such as code length, code weight and multiplicity index of modulation, which resulted in a guideline for proper selection of these parameters to be used for efficient system design.

8 Acknowledgments

Simin Khazraei acknowledges the financial support of the Iran Research Institute for Information and Communication Technology. The authors would also like to thank Seyed Ahmadreza Hosseini for his useful helps during this research.

9 References

1 Salehi, J.A.: 'Emerging optical code division multiple access communication systems', *IEEE Netw.*, 1989, **3**, (2), pp. 31–39
2 Bres, C.S., Prucnal, P.R.: 'Code-empowered lightwave networks', *J. Lightwave Technol.*, 2007, **25**, (10), pp. 2911–2921
3 Fouli, K., Maier, M.: 'OCDMA and optical coding: priciples, applications and challenges', *IEEE Commun. Mag.*, 2007, **45**, (8), pp. 27–34
4 Stock, A., Sargent, E.H.: 'The role of optical CDMA in access networks', *IEEE Commun. Mag.*, 2002, **40**, (9), pp. 83–87
5 Shalaby, H.M.H.: 'Performance analysis of optical synchronous CDMA communication systems with PPM signaling', *IEEE Trans. Commun.*, 1995, **43**, (2/3/4), pp. 624–634
6 Salehi, J.A.: 'Code division multiple-access techniques in optical fiber networks: Part I: fundamental principles', *IEEE Trans. Commun.*, 1989, **37**, (8), pp. 824–833
7 Salehi, J.A., Brackett, C.A.: 'Code division multiple-access techniques in optical fiber networks-Part II: systems performance analysis', *IEEE Trans. Commun.*, 1989, **37**, (8), pp. 834–842
8 Mashhadi, S., Salehi, J.A.: 'Code-division multiple-access techniques in optical fiber networks, part III: optical AND logic gate receiver structure with generalized optical orthogonal codes', *IEEE Trans. Commun.*, 2006, **54**, (8), pp. 1457–1468

9 Ghaffari, B.M., Matinfar, M.D., Salehi, J.A.: 'Wireless optical CDMA LAN: digital implementation analysis', *IEEE J. Selected Areas Commun.*, 2009, **27**, (9), pp. 1676–1686
10 Mashhadi, S., Salehi, J.A.: 'Optimum code structures for positive optical CDMA using normalized divergence maximization criterion', *IEEE Trans. Commun.*, 2008, **56**, (9), pp. 1414–1421
11 Shalaby, H.M.H.: 'Efficient use of PPM in spectral-amplitude-coding optical CDMA systems', *J. Lightwave Technol.*, 2012, **30**, (22), pp. 3512–3519
12 Khazraei, S., Pakravan, M.R.: 'Analysis of generalized optical orthogonal codes in optical wireless local area networks', *IEEE J. Select Areas Commun.*, 2009, **27**, (9), pp. 1579–1581
13 Khazraei, S., Pakravan, M.R., Aminzadeh-Gohari, A.: 'Analysis of power control for indoor optical wireless code-division multiple access networks using on-off keying and binary pulse position modulation', *IET Commun.*, 2010, **4**, (16), pp. 1919–1933
14 Shalaby, H.M.H.: 'A performance analysis of optical overlapping PPM-CDMA communication systems', *J. Lightwave Technol.*, 1999, **17**, (3), pp. 426–432
15 Shalaby, H.M.H.: 'Direct detection optical overlapping PPM-CDMA communication systems with double optical Hardlimiters', *J. Lightwave Technol.*, 1999, **17**, (7), pp. 1158–1165
16 Shoaie, M.A., Khazraei, S., Pakravan, M.R.: 'Performance analysis of slotted ALOHA random access packet-switching optical CDMA networks using generalized optical orthogonal codes and *M*-ary overlapping PPM signaling', *IEEE/OSA J. Opt. Commun. Netw.*, 2011, **3**, (7), pp. 568–576
17 Khazraei, S., Pakravan, M.R.: 'Generalized OOC assisted PPM and overlapping PPM, considering thermal noise and APD effect', *IEEE/OSA J. Opt. Commun. Netw.*, 2013, **7**, (5), pp. 696–703
18 Shiu, D., Kahn, J.M.: 'Differential pulse-position modulation for power-efficient optical communication', *IEEE J. Commun.*, 1999, **47**, (8), pp. 1201–1210
19 Zwillinger, D.: 'Differential PPM has a higher throughput than PPM for the band-limited and average power limited optical channel', *IEEE Trans. Inf. Theory*, 1998, **34**, (5), pp. 1269–1273
20 Sethakaset, U., Gulliver, T.A.: 'Performance of differential pulse-position modulation (DPPM) with concatenated coding over optical wireless communications', *IET Commun.*, 2008, **2**, (1), pp. 45–52
21 Mercier, H., Bhargava, V.K., Tarokh, V.: 'A survey of error-correcting codes for channels with symbol synchronization errors', *IEEE Commun. Surveys and Tutorials*, 2010, **12**, (1), 12, pp. 87–96
22 Shalaby, H.M.H.: 'Chip-level detection in optical code division multiple access', *J. Lightwave Technol.*, 1998, **16**, (6), pp. 1077–1087
23 Papoulis, A., Pillai, S.U.: 'Probability, random variables and stochastic processes' (Mc Graw Hill, New York, 2002, 4th edn.)
24 Raychaudhuri, D.: 'Performance analysis of random access packet switched code division multiple access systems', *IEEE Trans. Commun.*, 1981, **29**, (6), pp. 895–901
25 Carleial, A.B., Hellman, M.E.: 'Bistable behavior of aloha-type systems', *IEEE Trans. Commun.*, 1975, **23**, (4), pp. 401–410
26 Salehi, J.A., Chung, F.R.K., Wei, V.K.: 'Optical orthogonal codes: design, analysis and applications', *IEEE Trans. Inf. Theory*, 1989, **35**, (3), pp. 595–604
27 Ghaffari, B.M., Salehi, J.A.: 'Multiclass, multistage, and multilevel fiber-optic CDMA signaling techniques based on advanced binary optical logic gate elements', *IEEE Trans. Commun.*, 2009, **57**, (5), pp. 1424–1432
28 Verdu, S., Shamai, S.: 'Spectral efficiency of CDMA with random signaling', *IEEE Trans. Inform. Theory*, 1999, **45**, (2), pp. 622–640

10 Appendix

10.1 Appendix 1. M-*ary DPPM interference probability*

Fig. 14 shows all possible cases of interference between an interfering user and an *off* slot of the desired user. j represents beginning of a new symbol of the interfering user. It can take any value from the discrete set $\{0, -1, \ldots, -(M-1)\}$. i is the beginning of the *one* slot in the new symbol. An interference will happen when $i = 0$. Since symbols are equally probable to happen, i would be 0 with probability $1/M$. Since there are M cases and each case happens with probability $1/M$, we have

$$p_i = \frac{1}{M}\sum_{j=0}^{M-1}\frac{1}{M} = \frac{1}{M}$$

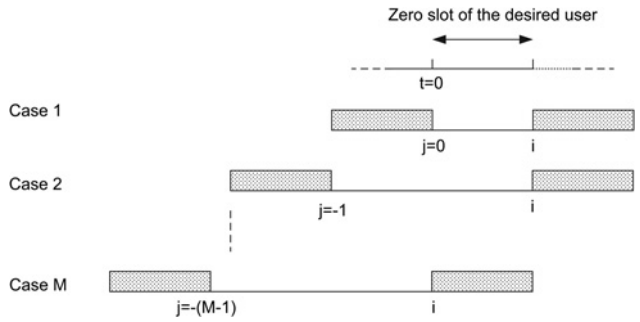

Fig. 14 *All the possible cases of interference*
j represents beginning of a new symbol of the interfering user

doi: 10.1049/iet-opt.2013.0076